

# Porous Au - TiO<sub>2</sub> aerogels nanoarchitectures for photodegradation processes

A. PETER<sup>a</sup>, L. BAIA<sup>b</sup>, M. BAIA<sup>b</sup>, E. INDREA<sup>c</sup>, F. TODERAS<sup>d</sup>, V. DANCIU<sup>e</sup>, V. COSOVEANU<sup>e</sup>, L. DIAMANDESCU<sup>f</sup>

<sup>a</sup>North University, Faculty of Science, Victoriei 76A, 430083, Baia-Mare, Romania

<sup>b</sup>Babes-Bolyai University, Faculty of Physics 400084, Cluj-Napoca, Romania

<sup>c</sup>National Institute for Research and Development of Isotopic and Molecular Technologies, Donath 71 – 103, RO-400293, Cluj-Napoca, Romania

<sup>d</sup>Institute for Interdisciplinary Experimental Research, Babes-Bolyai University, Treboniu Laurian 34, 400271, Cluj-Napoca, Romania

<sup>e</sup>Babes-Bolyai University, Faculty of Chemistry and Chemical Engineering, Arany Janos 11, 400028, Cluj-Napoca, Romania

<sup>f</sup>National Institute of Material Physics, P.O. Box MG-7, 77125 Bucharest, Romania

Porous nanoarchitectures based on TiO<sub>2</sub> aerogel and colloidal gold particles have been obtained by different synthesis routes: impregnation of TiO<sub>2</sub> aerogel with Au colloid, impregnation of TiO<sub>2</sub> gel with Au colloid and preparation of TiO<sub>2</sub> gel in the presence of Au colloid. The as prepared composites have been thermal treated at 500°C and their structural and morphological properties were investigated. The Raman spectra and XRD data demonstrated the anatase structure of the composite obtained by impregnation of TiO<sub>2</sub> aerogel with Au colloid and the mixed anatase-brookite structure of those obtained by impregnation of TiO<sub>2</sub> gel with Au colloid and by preparation of TiO<sub>2</sub> gel in the presence of Au colloid, respectively. TEM analyses suggest that the Au particles on the TiO<sub>2</sub> surface as individual particles, as well as clusters are present. The photocatalytic performances of the synthesized composites were tested in the salicylic acid photodecomposition process and it was found that they are strongly influenced by both anatase - brookite TiO<sub>2</sub> structure and Au nanoparticles dispersion on the TiO<sub>2</sub> surface.

(Received March 1, 2010; accepted May 26, 2010)

**Keywords:** Au / TiO<sub>2</sub> composites, sol-gel method, Raman spectroscopy, TEM, photocatalysis, salicylic acid.

## 1. Introduction

Aerogels are extremely porous materials generally obtained via sol-gel processing and supercritical drying [1, 2]. The very low density, high surface area, translucency or transparency to visible light and complex microstructure make them attractive candidates in photocatalytic applications [3]. Among them, TiO<sub>2</sub> aerogels are ones of the most preferred materials, due to their non-toxic nature and stability [4]. The improvement of the TiO<sub>2</sub> photocatalytic activity continues to be one of the most important aims of research in the field of photocatalysis. The surface modification of TiO<sub>2</sub> with noble metals (Au, Pt and Pd) has been proven to be an useful way to enhance its photocatalytic activity [5-17] by increasing the efficiency of charge carrier recombination rate, one of the disadvantages of TiO<sub>2</sub>. The photocatalytic activity of TiO<sub>2</sub> has been described to be strongly influenced by morphological and structural parameters, such as its crystal structure, specific surface area, porosity and surface hydroxyl group density [18, 19]. Sakthivel and co-workers [4] showed that metal - TiO<sub>2</sub> composites, obtained by impregnation of TiO<sub>2</sub> with metal salt solutions, were much efficiently photocatalysts in acid green 16 photodegradation processes towards pure TiO<sub>2</sub>.

Other authors [20, 21] demonstrated the importance of the Au / TiO<sub>2</sub> composites heat treatment for obtaining Au particles with diameter of about 2-3 nm and showed the potential of their use in the CO photo-oxidation process. Studies of CO oxidation on Au islands deposited on TiO<sub>2</sub> single crystal surfaces demonstrated a particle size effect with optimal activity for Au islands of 3.5 nm [22, 23]. Although this particle size effect is not well understood or proven to be the dominant factor, the correlation between “small” Au particle sizes and high CO oxidation activity, is by now considered as “well established” [20]. Pietron and co-workers [24] showed that a similar size of TiO<sub>2</sub> and Au particles allows the contact of an individual Au particle with multiple titania particles, increasing the photocatalytic efficiency of the Au / TiO<sub>2</sub> composites.

On the other hand, most of the above-mentioned studies confirm the anatase phase as the most efficient TiO<sub>2</sub> based photocatalyst. A previous work [25] performed in our laboratory was devoted to the obtaining of TiO<sub>2</sub> aerogel composites with pure anatase structure and high BET surface area. The best results have been established by changing the precursor's molar ratio and applying a post annealing at 500°C for 2 hours.

In this study we report on the synthesis and characterisation of novel nanoarchitectures based on TiO<sub>2</sub>

aerogel and Au colloidal particles with applications in salicylic acid photo-decomposition. Our interest was focused not only on evaluating the photocatalytic activity of the porous composites but also on finding the role played by their structure on the photodegradation rate of the salicylic acid.

## 2. Experimental

### 2.1. Preparation of TiO<sub>2</sub> aerogel - Au nanoparticle composites

TiO<sub>2</sub> aerogel - Au nanoparticle composites were prepared by three different routes, as presented in Table 1.

Table 1. Preparation routes of TiO<sub>2</sub> aerogel - Au nanoparticle composites.

	Preparation route	Composite ID
Impregnation of TiO <sub>2</sub> aerogel with Au colloidal particles	- immersion of TiO <sub>2</sub> aerogel for 3 days into the Au colloidal suspension - washing three times with water - drying in air at 100 °C	(a)
Impregnation of TiO <sub>2</sub> gel with Au colloidal particles	- immersion of TiO <sub>2</sub> gel for 3 days into the Au colloidal suspension - washing three times with ethanol - supercritical drying with CO <sub>2</sub> - heat treatment at 500 °C, for 2 h	(b)
Preparation of TiO <sub>2</sub> gels in the presence of Au colloidal particles	- mixing the precursors of TiO <sub>2</sub> gel (excepting the water) with Au colloidal suspension for obtaining Au-TiO <sub>2</sub> gels - gelation and aging 21 days - supercritical drying with CO <sub>2</sub> - heat treatment at 500 °C, for 2 h	(c)

In first route, TiO<sub>2</sub> aerogels were prepared by sol-gel method. The TiO<sub>2</sub> sols were obtained by mixing titaniumisopropoxide (IV) (Merck, 99.9%), with anhydrous ethanol (Fluka, 99.8%) as solvent, water and nitric acid reagent (Merck, 65%) as catalyst. The molar ratio of reactants was: [Ti(OC<sub>3</sub>H<sub>7</sub>)<sub>4</sub>] : [H<sub>2</sub>O] : [C<sub>2</sub>H<sub>5</sub>OH] : [HNO<sub>3</sub>] = 1 : 3.675 : 21 : 0.08. The TiO<sub>2</sub> gels were supercritical dried using liquid CO<sub>2</sub> in a SAMDRI – 790 A (Tousimis) at critical point dryer (T = 40 °C and p = 1400 psi). The obtained TiO<sub>2</sub> aerogels were transparent and were kept, for 3 days, in gold colloid, obtained by HAuCl<sub>4</sub> (Merck, 99.8%) reduction in the presence of sodium citrate (Merck). The reduction of Au<sup>3+</sup> to Au<sup>0</sup> on TiO<sub>2</sub> surface was obtained according to a standard procedure [24]. In the second route, the TiO<sub>2</sub> gels (obtained as mentioned above) were kept, for the same time, in the gold colloid. In the third route Au –TiO<sub>2</sub> gels were prepared by removing water with gold colloid. The used gold colloid volume was 40 mL. In the third route, the quantities of all reactants were calculated taking into consideration the used gold colloid volume. The gels obtained in the second and third routes were thermal treated at 500°C for 2 h, in a CARBOLLITE furnace, to obtain a TiO<sub>2</sub> crystalline phase, to remove organic residues and to achieve strong contacts between the TiO<sub>2</sub> and Au colloidal nanoparticles. The obtained composites were transparent, with a violet nuance. The authors intended to maintain constant the gold concentration, so due to the experimental work errors, the gold concentration in the obtained composites was in the range 0.37 – 0.38 ± 0.01% (0.37 % for composites (a) and (b) and 0.38% for composite (c)). This small gold variation does not influence the photoactivity of the obtained composites. The gold concentration was

spectrophotometrical measured using a Perkin Elmer FAAS 800 Flame Atomic Adsorption Spectrometer.

### 2.2. Characterization of TiO<sub>2</sub> aerogel-Au nanoparticle composites

The surface area of the as-prepared composites was determined by the Brunauer-Emmett-Teller (BET) method. A Sorptomatic, Thermo Electron Corporation system coupled with a Flatron L 1718S computer system was used. The partial pressure range was 0.05 < P/P<sub>0</sub> < 0.3. The nitrogen adsorption was carried out at 77 K. Before each measurement, the composites were heat treated at 333 K for 2 h.

A Nd-YAG laser (λ = 1064 nm) was employed for the recording of the composites Raman spectra. The FT-Raman spectra were recorded using a Bruker Equinox 55 spectrometer with an integrated FRA 106 Raman module, a power of 100 mW incidents on composite and a spectral resolution of 2 cm<sup>-1</sup>.

The phase content and the particle dimensions were determined from the XRD patterns recorded by means of a DRON X-ray powder diffractometer linked to a data acquisition and processing facility; CuK<sub>α</sub> radiation (λ = 1.540598 Å) and a graphite monochromator were used.

A JEOL 200 CX TEM operating at an accelerating voltage of 200 kV was employed to obtain bright (BF) and dark field (DF) images as well as the electron diffraction patterns of the composites. Particle sizes were measured from BF and DF images, whereas the phase content was investigated by using electron diffraction patterns. Composites were prepared by dipping a 3 mm holey

carbon grid into ultrasonic dispersed composite powder in ethanol.

The concentration of gold in all composites, determinate using an AAS 800 Atomic Adsorption Spectrometer, was appreciatively  $0.37 \pm 0.01\%$ .

### 2.3. Adsorption and photodegradation of salicylic acid on TiO<sub>2</sub> aerogel-Au nanoparticle composites

The adsorption properties and the photocatalytic activity of the TiO<sub>2</sub> aerogel - Au nanoparticle composites was established from the adsorption and degradation rate of salicylic acid used as a standard pollutant molecule [27]. In all adsorption and photodecomposition processes 0.05 g composite was used. The decrease in salicylic acid concentration ( $C_0 = 5.25 \times 10^{-4}$  M for all investigated composites) was monitored by UV-Vis spectroscopy ( $\lambda = 297$  nm). The composites immersed in salicylic acid solution were irradiated with a medium pressure Hg lamp HBO OSRAM (500 W). A Teflon photochemical cell with quartz window ( $S = 12$  cm<sup>2</sup>) and a capacity of 8 ml was also used. The distance between the photochemical cell and the lamp was about 30 cm. The working temperature was of 20-22°C and the solution pH was 5.3. Before UV irradiation as well as before UV-Vis measurements, the cell with the composite was kept in dark for 30 min in order to achieve the equilibrium of the adsorption-desorption process [27]. One should emphasize that throughout of the photo-decomposition process no shift of the UV band located at 297 nm was observed and no other new absorption band occurred. The color of Au/TiO<sub>2</sub> composites changes not after UV irradiation.

### 3. Results and discussion

The adsorption of salicylic acid onto TiO<sub>2</sub> aerogel - Au nanoparticle composites is evaluated by monitoring the disappearance of the 297 nm absorption band. The adsorption profiles of the prepared composites are displayed in Fig. 1 A.

As can be seen, an excellent adsorption occurs on the composite (b), a reduced adsorption of the salicylic acid being obtained on the composites (a) and (c). Onto TiO<sub>2</sub> aerogel, the salicylic acid adsorption occurs much intense than that on the composite (a) and Degussa P 25. These observations are confirmed by the adsorption rate constants (Table 2) which are calculated from the slope of the plot  $\ln(Q_t)$  vs. time ( $Q_t$  - current adsorbed quantity) after applying a linear fit [28].

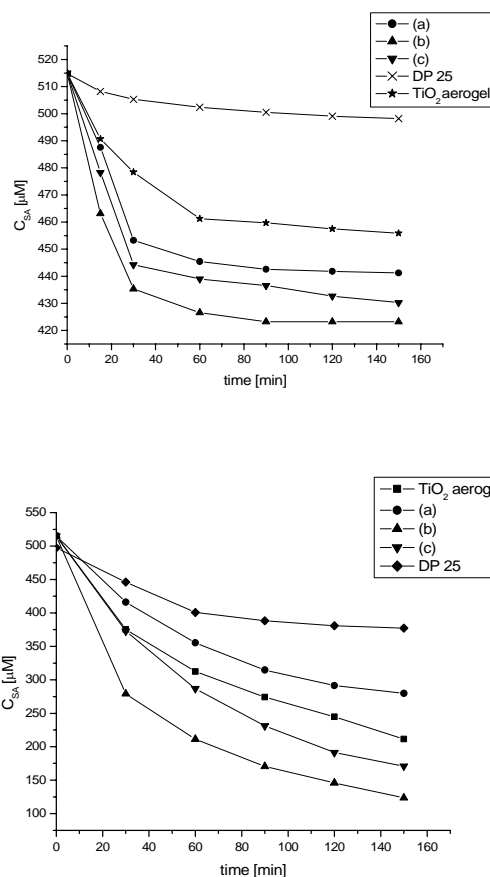


Fig. 1. Adsorption – A and photodegradation - B profiles of the salicylic acid on the TiO<sub>2</sub> aerogel-Au nanoparticle composites, in comparison with DEGUSSA P 25. (a) – composite obtained by impregnation of TiO<sub>2</sub> aerogel with gold colloid, (b) – composite obtained by impregnation of TiO<sub>2</sub> gel with gold colloid, (c) – composite obtained by TiO<sub>2</sub> gel preparation in the presence of the gold colloid.

The highest values of the adsorption rate constant of composites (b) and (c) are explained by the highest specific surface area of these composites (160 and 125 m<sup>2</sup>/g, respectively). Moreover, as can be seen in Figure 2, the composites with micro-mesoporous structure contain pores with 10 - 50 Å diameters. In composite (a), pores with 20 Å diameters are predominant. The composites (b) and (c) are more porous in contrast with composite (a), due to the prevalence of the pores with 30-50 Å diameters. Thus, the more intensely salicylic acid adsorption onto composite (b) is explained by both the higher specific surface area and the predominance of the pores with higher diameters.

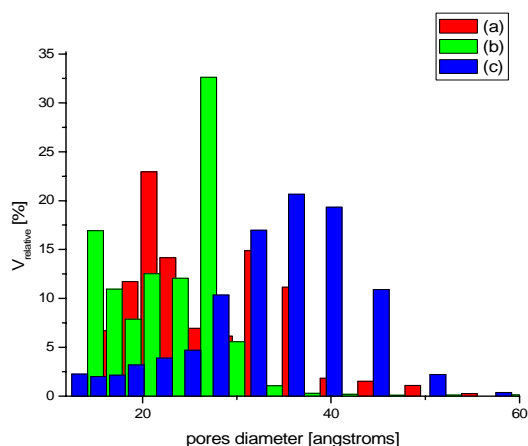


Fig. 2. Pore size distribution of the obtained composites. (a) – composite obtained by impregnation of TiO<sub>2</sub> aerogel with gold colloid, (b) – composite obtained by impregnation of TiO<sub>2</sub> gel with gold colloid, (c) – composite obtained by TiO<sub>2</sub> gel preparation in the presence of the gold colloid.

As can be seen in Fig. 1 B and in Table 2, the salicylic acid photodecomposition rate decreases in order: composite (b) > composite (c) > TiO<sub>2</sub> aerogel > composite (a) > Degussa P 25. The same order of decreasing was observed also in the adsorption process. The salicylic acid is photo-decomposed with the highest rate on the composites (b) and (c) than on the composite (a). On commercial Degussa P 25 powder, the salicylic acid photo-degradation was reduced in comparison with that recorded on the TiO<sub>2</sub>-Au composites and TiO<sub>2</sub> aerogel.

The photo-decomposition rate constants (Table 2) were obtained from the slope of the plot  $\ln(C_0/C)$  vs time after applying a linear fit [29]. These results can be correlated with the adsorption ones, concluding that the salicylic acid is well adsorbed onto composite (b) and less on composite (a). However, it could be emphasized the overall improvement of the photocatalytic performances obtained for the as-prepared composites (reaction rate constants were 4.8, 3.9 and 2.5 times higher for composites (b), (c) and (a), respectively) in comparison with that of the commercial Degussa P 25 achieved in similar experimental conditions. In contrast, only by TiO<sub>2</sub> gel impregnation in gold colloid (composite (b)) and TiO<sub>2</sub> gel preparation in the presence of the gold colloid (composite (c)) the photodegradation rate constant increases toward TiO<sub>2</sub> by 1.56 and 1.26 times respectively.

Table 2. Salicylic acid adsorption and photodegradation rate constants, crystalline phase composition, TiO<sub>2</sub> particle diameter and specific surface area of the investigated composites (A - anatase, B - brookite).

Compo- site ID	S <sub>BET</sub> (m <sup>2</sup> /g)	k <sub>ads.</sub> x 10 <sup>3</sup> [min <sup>-1</sup> ]	k <sub>photo.</sub> x 10 <sup>3</sup> [min <sup>-1</sup> ]	Crystalline phase Composition (%)		Particle size (nm)	
				A	B	A	B
(a)	93	0.04	6.17	100	-	15	-
(b)	160	0.31	12.02	79	21	12	9
(c)	125	0.28	9.75	60.5	39.5	21	10
TiO <sub>2</sub> aerogel	101	0.09	7.7	100	-	9.6	-
Degussa P 25	50	0.009	2.5	80	-	20	-

The Raman spectra of TiO<sub>2</sub> aerogel-Au nanoparticle composites are displayed in Figure 3. As can be seen, the TiO<sub>2</sub> anatase crystalline phase builds up the structure of the porous composites annealed at 500°C, giving rise to well-defined bands around 146, 197, 399, 517 and 639 cm<sup>-1</sup>. These five peaks correspond to the well-known five fundamental vibrational modes of the anatase phase with the symmetries of E<sub>g</sub>. The E<sub>g</sub>, B<sub>1g</sub>, A<sub>1g</sub>, B<sub>1g</sub>, respectively [30]. A close analysis of the spectra reveals the presence of other three very small Raman bands around 245, 320 and 365 cm<sup>-1</sup> (denoted by stars), especially in the spectrum of the composite (c). Such spectral features were previously observed [31-34], when ultrafine TiO<sub>2</sub> powders with grain sizes around 10 nm were investigated, and were attributed to the existence of brookite phase. Since the above-mentioned Raman characteristics are very similar in all recorded spectra XRD measurements have been further performed. It should be mention that normally gold nanoparticles do not give rise to any Raman signal. The XRD results indicate the presence of a biphasic anatase and brookite structure for the composites (b) and (c), while a unique anatase

phase was found for the composite (a) (not shown). The particle size of anatase and brookite crystallites was determined together with their relative abundance in the studied composites (Table 2).

No reflections due to polycrystalline gold are detected in the XRD patterns, pointing out the low metal content [35]. The largest anatase particles (average size) were found in the composite (c), while the smallest ones are incorporated in the composite (b), which shows the highest photodecomposition rate constant. One observes that the composites (b) and (c), in which both anatase and brookite phases are in contact with Au nanoparticles, show a higher photocatalytic activity in comparison with composite (a) and TiO<sub>2</sub> aerogel, in which only anatase phase is in contact with gold particles. Yu and co-workers [36] explained the improvement of TiO<sub>2</sub> photocatalytic activity in the case of Au-TiO<sub>2</sub> composites by taking into consideration that the coupling of metal / anatase, metal / brookite allowed the migration of photogenerated electrons from anatase or brookite phases to metal and significantly retarded the recombination of the electron and hole pairs in anatase or brookite.

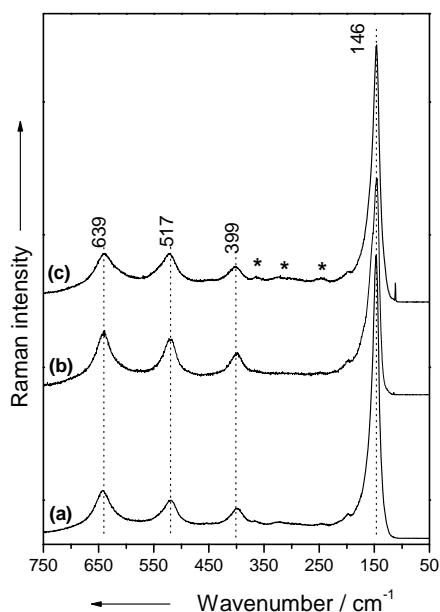


Fig. 3. Raman spectra - A of the prepared TiO<sub>2</sub> aerogel-Au nanoparticle composites. (a) – composite obtained by impregnation of TiO<sub>2</sub> aerogel with gold colloid, (b) – composite obtained by impregnation of TiO<sub>2</sub> gel with gold colloid, (c) – composite obtained by TiO<sub>2</sub> gel preparation in the presence of the gold colloid.

Comparing the brookite average particles size of the composites (b) and (c) one observes that the composite (b) with the smaller brookite average particles size (9 nm) have a higher photoactivity than composite (c) with brookite average particles of 10 nm. It seems that the higher photocatalytic activity of the composite (b) is due to the presence of brookite phase corroborated with other characteristics (see below). This statement is in agreement with the literature studies [34] sustaining that the photocatalytic activity of the composites increases with the brookite particles growth.

According to TEM pictures analysis, the composite (a) (Figure 4 A) contains a relative high number of fine gold particles (5-8 nm diameter) incorporated in the TiO<sub>2</sub> anatase network. The TiO<sub>2</sub> anatase particles are highest than those of gold, having diameters between 10 and 15 nm. The diffraction image from Figure 4 A shows diffractions spots due to the gold particles presence. The Au particles are relative homogeneous dispersed into the TiO<sub>2</sub> phase, but in some areas (not shown), the Au colloidal particles were agglomerate into thin-plates, excessive growth, behaviour that leads to a diminishing of the contact points between the TiO<sub>2</sub> and Au nanoparticles that consequently can cause a decrease of the photodegradation rate.

The TEM image (Fig. 4 B) shows that the composite (b) have a biphasic structure (anatase and brookite) (confirmed also by Raman and XRD results), in which the Au colloidal nanoparticles are well dispersed in

comparison with composite (a) (figure 4 A), some of them being crystallized. The anatase and gold particles diameters were about 10 nm and the brookite particles dimensions are highest (12 nm).

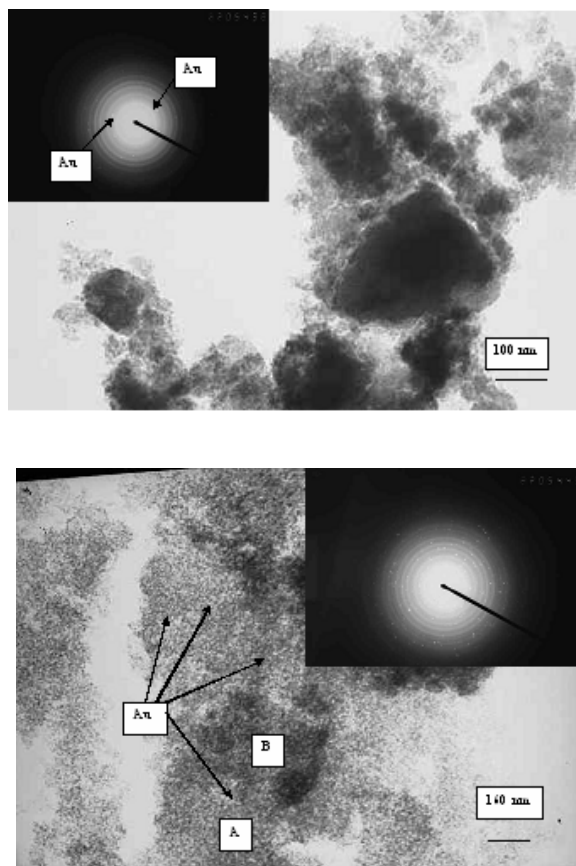
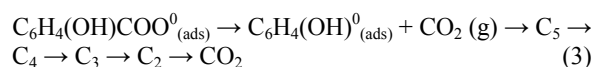
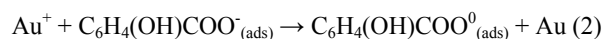
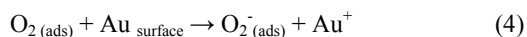


Fig. 4. TEM image of the composites obtained by impregnation of TiO<sub>2</sub> aerogel with gold colloid (composite a) – A, by impregnation of TiO<sub>2</sub> gel with gold colloid (composite b) (A-anatase, B-brookite) – B.

The composite (c) contains amorphous TiO<sub>2</sub> phases (TEM image not shown), but relative well crystallized gold particles. The gold colloid have not been incorporated into the TiO<sub>2</sub> network, in this material type.

The homogeneity of the Au particles dispersion on the TiO<sub>2</sub> surface can positively influence the photocatalytic performances of composites (b) and, in contrast with composite (a), where the gold particles are agglomerated into clusters. This fact could be explained taking into consideration the mechanism of charge carriers transfer (reactions 1-5) [37].





The photogenerated holes combine with Au particles on TiO<sub>2</sub> surface generating Au<sup>+</sup> ions (reaction 1), which can react with salicylic acid anions adsorbed onto TiO<sub>2</sub> surface, generating salicylic acid radicals (reaction 2), which are decarboxylated with formation of carbon dioxide (reaction 3). On the other hand Au particles can combine with adsorbed O<sub>2</sub>, generating O<sub>2</sub><sup>-</sup> anions and Au<sup>+</sup> cations (reaction 4). Au<sup>+</sup> ions will attack a new salicylic acid anion (reaction 2). The agglomeration of Au particles into clusters, decreases the number of Au particles available for reactions, so the photodegradation rate of the composite (a) is significantly reduced.

By corroborating the results derived from TEM, Raman and XRD analyses with the photodegradation rates it can be concluded that the formation of the TiO<sub>2</sub> anatase crystalline phase is not the only important characteristic that contributes to the improvement of the photocatalytic efficiency of the TiO<sub>2</sub>-Au nanocomposite systems. Thus, besides the size of Au and TiO<sub>2</sub> nanoparticles, other important parameters like homogeneous dispersion of Au particles on the TiO<sub>2</sub> surface and the presence of a mixed anatase - brookite phase could positively influence the photocatalytic performances.

#### 4. Conclusions

In this study the preparation of porous nanoarchitectures Au - TiO<sub>2</sub> composites, by three different preparation routes (impregnation of TiO<sub>2</sub> aerogel with Au colloid, impregnation of TiO<sub>2</sub> gel with Au colloid and preparation of TiO<sub>2</sub> gel in the presence of Au colloid) was reported. The obtained composites were morpho-structural characterized by BET method, Raman spectroscopy, XRD and TEM. The salicylic acid adsorption on the obtained composites and its photocatalytic degradation were evaluated under different experimental conditions. Among the investigated composites, those obtained by impregnation of the TiO<sub>2</sub> gel with gold colloid and by preparation of the TiO<sub>2</sub> gel in the presence of the gold colloid, thermally treated at 500°C, contain a mixture of anatase - brookite phase, present the highest specific surface area and are characterized by a high dispersion of Au particles. These factors are considered responsible for the enhancement of the photocatalytic activity observed in the case of above mentioned composites.

#### References

- [1] S. S. Kisler, *J. Phys. Chem.* **36**, 52 (1932)
- [2] N. Hüsing, U. Schubert, *Angew. Chem. Int. Ed.* **37**, 22 (1998)
- [3] G. Dagan, M. Tomkiewicz, *J. Phys. Chem.* **97**(49), 12651 (1993)
- [4] S. Sakthivel, M. V. Shankar, M. Palanichamy, B. Arabindoo, D. W. Bahnemann, V. Murugesan, *Water Res.* **38**, 3001 (2004)
- [5] R. S. Sonawane, M. K. Dongare, *Mol J Catal A* **243**, 68 (2006)
- [6] A. Orlov, D.A. Jefferson, N. Macleod, R. M. Lambert, *Catal Lett.* **92**, 41 (2004)
- [7] H. Li, Z. Bian, J. Zhu, Y. Huo, H. Li, Y. Lu, *J. Am. Chem. Soc.* **129**, 4538 (2007)
- [8] S. C. Chan, M. A. Barteau, *Langmuir* **21**, 5588 (2005)
- [9] P. V. Kamat, *J. Phys. Chem. B* **106**(32), 7729 (2002)
- [10] P. V. Kamat, M. Flumiani, A. Dawson, *Coll. & Surf. A: Physicochem. & Eng. Aspects* **202**, 269 (2002)
- [11] V. Subramanian, E. E. Wolf, P. V. Kamat, *J. Am. Chem. Soc.* **126**, 4943 (2004)
- [12] A. Orlov, D.A. Jefferson, M. Tirkov, R. M. Lambert, *Catal. Commun.* **8**, 821 (2007)
- [13] P. D. Cozzoli, M. L. Curri, A. Agostano, *Chem. Commun.* **25**, 3186 (2005)
- [14] P. D. Cozzoli, E. Fanizza, R. Comparelli, M. L. Curri, A. Agostano, *J. Phys. Chem. B* **108**, 9623 (2004)
- [15] A. Dawson, P.V. Kamat, *J. Phys. Chem. B* **105**, 960 (2001)
- [16] S. L. Cao, K. L. Yeung, J. K. C. Kwan, P. M. T. To, S. C. T. Yu, *Appl. Catal. B* **86**, 127 (2009)
- [17] K. Y. Ho, K. L. Yeung, *Gold Bull.* **40**, 15 (2007)
- [18] X. Chen, S. S. Mao, *Chem. Rev.* **107**, 2891 (2007)
- [19] S. Sakthivel, M. C. Hidalgo, D. W. Bahnemann, S-U. Geissen, V. Murugesan, A. Vogelwohl, *Appl. Catal.* **63**, 31 (2006)
- [20] S. H. Overbury, L. Ortiz-Soto, H. Zhu, B. Lee, M. D. Amiridis, S. Dai, *Catal. Lett.* **95**(3-4), 99 (2004)
- [21] Y. Zhu, Y. Zhou, X. Lu, X. Feng, Z. Yang, *Catal. Lett.* **127**, 406 (2009)
- [22] M. Valden, S. Pak, X. Lai, D.W. Goodman, *Catal. Lett.* **56**, 7 (1998)
- [23] M. Valden, X. Lai, D.W. Goodman, *Science* **281**, 1647 (1998)
- [24] J. J. Pietron, R. M. Stroud, D. R. Rolison, *NanoLetters* **5**, 545 (2002)
- [25] L. Baia, M. Baia, A. Peter, V. Cosoveanu, V. Danciu, *J. Optoelectron. Adv. Mater.* **9**(3), 668 (2007)
- [26] C. D. Keating, M. D. Musick, M. H. Keefe, M. J. Natan, *J. Chem. Educ.* **76**(7), 949 (1999)
- [27] M. Tomkiewicz, *Catal. Today* **58**, 115 (2000)
- [28] S. M. Ould-Mame, O. Zahraa, M. Bouchy, *Int. J. Photoenergy* **2**, 59 (2000)
- [29] A. Peter, V. Danciu, V. Cosoveanu, Z. Moldovan, E. Indrea, G. Nutiu, L. Baia, I. Rosu, *Proceeding of the Conference Innovations In The Field Of Water Supply, Sanitation And Water Quality Management* **103** (2005)
- [30] L. Baia, A. Peter, V. Cosoveanu, E. Indrea, M. Baia, J. Popp, V. Danciu, *Thin Solid Films* **511-512**, 512 (2006)
- [31] I. H. Zhang, C. K. Chan, J. F. Porter, W. Guo, *J. Mater. Res.* **13**, 2602 (1998).

- [32] G. Busca, G. Ramis, J. M. G. Amores, V. S. Escribano, P. Piaggio, *J. Chem. Soc. Faraday Trans.* **90**, 3181 (1994)
- [33] M. Gotic, M. Ivanda, A. Sekulic, S. Music, S. Popovic, A. Turkovic, K. Furic, *Mater. Lett.* **28**, 225 (1996)
- [34] V. Danciu, L. Baia, V. Cosoveanu, M. Baia, F. Vasiliu, L. Diamandescu, C. M. Teodorescu, M. Feder, J. Popp, *Optoelectron. Adv. Mater.-Rapid Comm.* **2**(2), 76 (2008).
- [35] M. A. Centeno, M. C. Hidalgo, M. I. Dominguez, J. A. Navio, J.A. Odriozola, *Catal. Lett.* **123**, 198 (2008)
- [36] J. Yu, J. Xiong, B. Cheng, S. Liu, *Appl. Catal. B* **60**, 211 (2005)
- [37] F. B. Li, X. Z. Li, *Appl. Catal. A* **228**, 15 (2002)

\*Corresponding author: peteranca@yahoo.com